# $A_g$ Raman modes and ion-position dependence of the electronic structures of $YBa_2Cu_3O_7$ and $YBa_2Cu_4O_8$ from first principles

H. Khosroabadi, B. Mossalla, and M. Akhavan*
*Magnet Research Laboratory (MRL), Department of Physics, Sharif University of Technology, P.O. Box 11365-9161, Tehran, Iran*
(Received 6 December 2006; revised manuscript received 11 June 2007; published 9 August 2007)

Calculations of the frozen phonon for $A_g$ Raman modes of the superconducting $YBa_2Cu_3O_7$ and $YBa_2Cu_4O_8$ systems have been carried out using the pseudopotential density functional theory in the local density approximation employing the VASP code. The eigenvalues and eigenvectors of the $A_g$ Raman modes for the two systems have been calculated and compared with other experimental and computational studies. Electronic band structure and total density of states have been calculated for all the bare $A_g$ modes for both systems. By calculating the changes in the bands intersecting the Fermi energy by ionic displacements, the ionic dependence of the electronic band structure in each of the $A_g$ Raman modes and the relative importance of each mode have been investigated. This study suggests a strong ionic position dependence of the electronic band structure, and hence an indirect evidence for strong electron-phonon interaction in these systems.

DOI: 10.1103/PhysRevB.76.054508 PACS number(s): 74.25.Kc, 74.25.Jb, 74.72.Bk

## I. INTRODUCTION

More than two decades after the discovery of high temperature superconductors (HTSCs),[1] there is yet no consensus on a complete microscopic theory for explaining the different aspects of this phenomenon. However, in recent years, there has been an intense debate about which of the electronic correlation or electron-phonon interaction has the crucial role in formation of the superconducting state in HTSCs.[2,3] The early belief, deduced from some experimental facts, such as linear temperature dependence of resistivity in the wide range of temperature,[4] large antiferromagnetic transition temperature in undoped compound, and small value of isotope coefficient in optimally doped systems,[5] was that the electron-phonon interaction plays a secondary role in the physics and, as a result, in the superconducting state of HTSCs.

However, recent experimental[6,7] and computational[8] studies indicate that electron-phonon interaction could have a crucial role in the mechanism of superconductivity of HTSCs. Inelastic neutron scattering[9] and inelastic x-ray scattering[10] experiments indicate strong doping and momentum dependence of phonon softening, especially for the bond stretching mode, suggesting a substantial coupling of the phonons with the doped holes.[11] A large kink in the hole band dispersion, observed by the angle resolved photoemission spectroscopy,[6] indicates a strong coupling of the holes with a bosonic mode (claimed to be phonon mode[3,6,7]) with 70 meV energy. The observed unconventional isotope effects of different characteristics of these compounds, such as superconducting transition temperature ($T_c$), magnetic penetration depth, pseudogap, and antiferromagnetic ordering temperatures, strongly support the importance of lattice vibrations in the physics of HTSCs.[12] Computational studies also indicate a strong distance dependence of the hopping and Coulomb integrals[13] and large electron-phonon coupling constant[14] which results in a strong electron-phonon coupling in HTSCs. It has been also shown that the renormalization of electron-phonon interaction by the electronic correlations could explain the anomalous behavior of transport experiments and introduces a large coupling constant for producing high $T_c$,[2] though more studies are needed to clarify better this interesting subject.

Some useful data needed for these studies are the phonon dispersion relation, i.e., the eigenvalues and eigenvectors of the phonon modes. The local density functional theory has been successful in calculating these quantities for HTSCs at least at the center of the Brillouin zone ($q=0$), even in the strong correlation region where the compounds are antiferromagnetic insulator and band picture has some overestimations.[15,16] Also, this method has been used successfully to calculate and explain the experimental data of the optical[17,18] and x-ray absorption[19] spectra, electron-phonon interaction,[14] and Raman resonant scattering[20,21] of HTSCs.

In the previous studies, different approaches such as linear augmented plane waves (LAPW)[16] and linear muffin-tin orbitals[22] have been used to calculate the electronic and phonon properties of HTSCs. The computational studies have been faced with some challenges which have limited the studies. Their most important problems resulted from the intrinsic complex structure of HTSCs such as large unit cell with large number of ions, including the heavy rare earth and Cu ions with large number of electrons and localized $d$ or $f$ orbitals, etc. So, one important criterion and challenge in these studies is to choose a suitable method, in spite of its best efficiency and obtaining reliable results, to perform the calculations with the least time and computational facilities.

In our previous studies,[23] it was indicated that pseudopotential approach could be used to overcome this barrier to do large computational projects. We indicated that the results of electronic structure and high pressure calculations of Vienna *ab initio* simulation package (VASP) code are in good agreement with the experimental and computational data. The VASP pesudopotential code not only makes reliable results but also saves considerably time and computational facilities, with respect to some other full-potential codes. It is especially more beneficial when the calculation is done for supercell (due to the unperiodicity, for example, with considering doping) or when large number of calculations has to be car-

 

ried out for calculating a property (such as phonon) of the complex structures of HTSC systems.

Using pseudopotential method is usually faster than the full-potential methods and the doubt for probably underestimation of using the pseudopotential in comparison with full potentials has been removed by some studies.[23,24] Although some recent full-potential codes have been improved such that they could do the calculations with saving time and computational facilities (such as WIEN2K based on the LAPW method[25]), this study suggests the VASP as an alternative method for these calculations. In this study, the accuracy of the code is discussed for the Raman calculations.

Another useful calculation is determination of the ionic position dependence of electronic band structure in these ionic compounds which gives a hint on the role of phonons in their properties. Some examples of such studies are the Raman intensities and electron-phonon coupling constant calculations for $YBa_2Cu_3O_7$ (Y123) (Ref. 20) and LSCO (Ref. 14), but as far as we know there is no published complete results for $YBa_2Cu_4O_8$ (Y124). In addition, this study is focused on another view to shed light on the role of electron-phonon coupling in these systems, which is not considered well in other studies.

In this study, the eigenvectors and eigenfrequencies of the $A_g$ Raman modes and the ionic position dependence of the electronic band structure (BS) for Y123 and Y124 systems in the local density approximation (LDA) have been calculated and compared with the other computational and experimental data. These results could be useful in estimating the coupling of electrons with phonons in these systems.

## II. COMPUTATIONAL DETAILS

The total energy calculations have been performed using *ab initio* pseudopotential in the local density functional theory. We have used the VASP computational code,[26,27] which has proved to be a suitable computational code for Y123.[23] The initial lattice parameters for the calculation have been taken from the experimental data as $a=3.83$ Å, $b=3.88$ Å, and $c=11.68$ Å for Y123, and $a=3.85$ Å, $b=3.87$ Å, and $c=27.25$ Å for Y124.[28] Due to the presence of two CuO adjacent chains in Y124, the unit cell of this system is twice larger than the one in Y123 with $c=27.25$ Å. Subsequently, the equilibrium volume and lattice parameters for the two systems have been determined by Murnaghan fitting of energy-volume curve. The initial $z$ ionic positions for Y123 have been taken, respectively, as 0.159 72, 0.182 58, 0.353 65, 0.3789, 0.3798, for O(4), Ba, Cu(2), O(3), and O(2) from our previous calculations.[23] The data for Y124 have been taken from experiment[28] as 0.051, 0.053, 0.062, 0.135, 0.146, 0.213, and 0.218 for O(2), O(3), Cu(2), Ba, O(4), Cu(1), and O(1), respectively. To optimize the ionic positions, ion relaxation has been carried out manually by the change of ionic positions in the force direction to minimize the ionic forces as small as 0.01 eV/Å.

The atomic pseudopotential for the Y $4d$ and $5s$, Ba $5p$ and $6s$, Cu $3d$ and $4s$, and O $2s$ and $2p$ orbitals have been employed from the VASP library files. The suitable cutoff energy and $k$-point sampling in the irreducible Brillouin zone are determined to be 400 eV for both systems and $50k$ and $25k$ (corresponding to $9\times9\times3$ and $9\times9\times2$ mesh in the Monkhorst-Pack scheme[29]) for Y123 and Y124, respectively. The numbers of grid points in the fast Fourier transforms mesh, $N_{GX}$, $N_{GY}$, and $N_{GZ}$, have been selected, respectively, to be 30, 30, and 90 for Y123, and 28, 28, and 180 for Y124, to avoid wrap error. Charge density calculations have been carried out in $40\times40\times120$ and $40\times40\times270$ mesh points in the unit cell of Y123 and Y124, respectively.

To calculate the frozen phonon frequencies at $q=0$, one of the Ba, Cu(2), O(2), O(3), and O(4) ions [plus Cu(1) and O(1) in Y124] has been displaced in the $c$ direction by step $0.002c$ in the $0.010c$ range ($0.001c$ in the $0.006c$ range for Y124) around its equilibrium position in the experimental lattice parameters, while other ions have been remained fixed at their equilibrium positions. The total energy has been converged in each calculation to better than $10^{-4}$ eV/(unit cell). Then, the electronic BSs have been calculated in the high symmetric lines of $k_z=0.0$ plane of the irreducible Brillouin zone for equilibrium ionic positions and for each displacement of the ionic position in each bare phonon mode.

## III. RESULTS AND DISCUSSION

The equilibrium lattice parameters (with constant $c/a$ and $b/a$ ratios) and volume have been derived as $a=3.786$ Å, $b=3.836$ Å, $c=11.546$ Å, and $V=167.67$ Å$^3$ for Y123, and $a=3.806$ Å, $b=3.826$ Å, $c=26.937$ Å, and $V=392.19$ Å$^3$ for Y124 by the Murnaghan fitting of the total energy-volume data. From this calculation and our previous study,[23] it is found that the data fit well with the Murnaghan equation of state in these large anisotropic systems. Comparing the equilibrium lattice parameters with the experimental data indicates a relative difference as small as −1.14% for both systems. Corresponding values for volume are −3.5% and −3.4% for Y123 and Y124 systems, respectively. It is interesting that this underestimation is also better than the value obtained by the full-potential method. For example, the LAPW method in the LDA gives −6% (Ref. 16) and −5% (Ref. 22) for Y123, −5.7% and −6.4% for Pr123 and Gd123,[30] and −4.3% for $La_2CuO_4$.[31] By comparison with our previous study,[30] the time for this calculation is reduced by a factor of 6–8 times with respect to the LAPW calculation, with also having 1 order of magnitude better in energy convergence. Although using generalized gradient approximation (GGA) in LAPW method could improve the underestimation, the difficulty in the energy convergency and the increasing computational time make yet the VASP code as a suitable computational code.

The relative $z$ coordination of the equilibrium ionic positions of O(2), O(3), Cu(2), Ba, O(4), Cu(1), and O(1) ions of Y124 have been derived to be 0.051 87, 0.051 92, 0.061 25, 0.135 54, 0.145 65, 0.212 80, and 0.218 58, respectively. These data are in good agreement with the experimental data.[28] The uncertainties of these values in our calculation are smaller than $10^{-4}$ ($2\times10^{-4}$ for Y123).[23] Bulk moduli ($B$) for Y123 and Y124 have been derived to be 128.3 and 124 GPa, respectively, which are close to the reported data for similar systems.[32,33] Again, the value of $B$ obtained by

TABLE I. The eigenvalues and eigenvectors of the $A_g$ Raman-active modes of Y123.

| | | Eigenvectors | | | | |
|---|---|---|---|---|---|---|
| $A_g$ mode | Freq. ($cm^{-1}$) | Ba | Cu(2) | O(2) | O(3) | O(4) |
| Ba | 103 | 0.55 | 0.81 | 0.13 | 0.12 | −0.08 |
| Cu(2) | 134 | −0.56 | 0.80 | 0.09 | 0.10 | −0.14 |
| O(2)−O(3) | 353 | −0.02 | 0.00 | 0.79 | −0.61 | 0.04 |
| O(2)+O(3) | 394 | −0.01 | −0.03 | 0.52 | 0.70 | 0.49 |
| O(4) | 450 | 0.01 | 0.05 | −0.33 | −0.36 | 0.87 |

VASP is in better agreement with the experimental value ( ~115 GPa) relative to the results of LAPW in the LDA with values about $B=142-157$ GPa for Y123, Pr123, and Gd123.[16,30] Although the GGA could improve the results in comparison with the VASP results, it has more difficulty in the energy convergency and increasing the computational time. So, these results not only indicate the capability of the VASP code for determining the equilibrium structural and internal parameters and bulk modulus of HTSCs but also they have been improved relative to the full-potential LAPW method in addition to saving considerable computational time.

### A. Phonon spectrum

We have calculated the dynamical $K$ matrix $[K_{ij}=(M_iM_j)^{-1/2}\partial^2 E_{\text{tot}}/\partial z_i \partial z_j$ where $M$ and $z$ indicate the ionic mass and the $c$ direction position of the, $i,j$th ion] for Ba, Cu(2), O(2), O(3), and O(4) ions for Y123 [in addition to Cu(1) and O(1) for Y124] which are Raman-active modes in these systems. The diagonal and off diagonal elements have been derived from fitting of the energy-position and force-position (linear relation) data, respectively. The bare phonon frequencies have been derived to be 120, 129, 375, 386, and 436 $cm^{-1}$ for Ba, Cu(2), O(2), O(3), and O(4) oscillations in Y123, and 104, 255, 130, 579, 372, 382, 489 $cm^{-1}$ for Ba, Cu(1), Cu(2), O(1), O(2), O(3), and O(4) oscillations in Y124, respectively. The eigenvalues and eigenvectors of $A_g$ Raman modes of Y123 and Y124 are presented in Tables I and II, respectively.

For the $A_g$ modes of Y123, the Ba and Cu(2) ions in the first two of the five $A_g$ modes, known as Ba and Cu(2) modes, have been considerably mixed together while their mixing with the oxygen ions is low. In the Ba mode, the Cu(2) and Ba ions oscillate in the same phase, while in the Cu(2) mode both ions oscillate in the opposite phase. The O(2) and O(3) bare phonon modes (with nearly same positions and hence degenerate bare phonon energies) change into two odd and even combinations of these ions, shown as O(2)−O(3) and O(2)+O(3), respectively. The odd O(2)−O(3) mode with lower energy contains the oscillation of O(2) and O(3) ions in the opposite phase and are decoupled from other ions. While, in the even O(2)+O(3) mode, the O(2) and O(3) ions are oscillated in the same phase and coupled with O(4) ion in the same phase. The lower frequency of the O(2)−O(3) mode relative to the O(2)+O(3) mode could be understood simply but crudely based on different changes of electrostatic energy due to the interaction of Cu(2) and oxygen ions in these modes. In the O(2)+O(3) mode, due to the buckling of the $CuO_2$ plane, both of the oxygen ions become far or near the Cu(2) ions together. So the electrostatic energy versus ionic position in this mode is changed faster than in the O(2)−O(3) mode where the two oxygen ions move in opposite directions, and the distance of one oxygen ion with Cu(2) ion decreases while another one increases. In the fifth mode with the highest phonon energy in this system, O(4) ion has a dominant amplitude and couple to the O(2) and O(3) ions in the opposite phase. Good agreement between our calculation and other studies has been found.[16,30,34] In this relation, a detailed comparative study has been previously published for Gd123 and Pr123 systems.[30]

The above results for Y123 are considerably different for the Y124 system, which due to the presence of two CuO chains has seven $A_g$ Raman-active modes: Five modes, similar to the ones in Y123, and two extra modes from the Cu(1) and O(1) oscillations. In this system, also the heavy Ba and Cu(2) ions decouple from the light oxygen ions and Cu(1), while the Cu(1) ion in the Cu(1) mode is not mixed with the Cu(2) and Ba ions. In the first mode, Ba ion is coupled with the Cu(2) ion in opposite phase, while in the second mode they oscillate in the same phase. In the third mode, the Cu(1) ion has the dominant amplitude and couples with the O(4) ion. In the fourth mode, the O(2) and O(3) ions couple in the

TABLE II. The eigenvalues and eigenvectors of the $A_g$ Raman-active modes of Y124.

| | | Eigenvectors | | | | | | |
|---|---|---|---|---|---|---|---|---|
| $A_g$ mode | Freq. ($cm^{-1}$) | Ba | Cu(1) | Cu(2) | O(1) | O(2) | O(3) | O(4) |
| Ba | 96 | 0.79 | −0.02 | −0.60 | 0.02 | 0.06 | 0.05 | −0.11 |
| Cu(2) | 121 | 0.32 | −0.13 | 0.89 | 0.01 | −0.19 | −0.18 | 0.19 |
| Cu(1) | 250 | 0.05 | 0.96 | 0.12 | 0.13 | 0.10 | 0.04 | −0.19 |
| O(2)−O(3) | 346 | 0.00 | −0.05 | 0.03 | 0.06 | −0.49 | 0.67 | −0.55 |
| O(2)+O(3) | 404 | 0.01 | −0.07 | 0.09 | −0.02 | 0.62 | 0.75 | −0.21 |
| O(4) | 490 | 0.01 | 0.05 | −0.02 | −0.23 | 0.14 | 0.15 | 0.95 |
| O(1) | 585 | 0.00 | −0.02 | −0.01 | 0.97 | 0.04 | 0.05 | 0.23 |

TABLE III. The eigenvalues of the $A_g$ Raman-active modes of Y123 and Y124 in comparison with the reported computational and experimental data.

| | Freq. ($cm^{-1}$) | | | | | |
|---|---|---|---|---|---|---|
| $A_g$ mode | Y123[c] | Y123 (Expt.)[a] | Y123 (Comp.)[b] | Y124[c] | Y124 (Expt.)[d] | Y124 (Comp.)[e] |
| Ba | 103 | 110–119 | 95–123 | 96 | 103 | 89 |
| Cu(2) | 134 | 145–159 | 127–147 | 121 | 150 | 169 |
| Cu(1) | ··· | ··· | ··· | 250 | 247 | 270 |
| O(2)−O(3) | 353 | 330–336 | 317–338 | 346 | 340 | 393 |
| O(2)+O(3) | 394 | 435–440 | 387–422 | 404 | 439 | 426 |
| O(4) | 450 | 493–500 | 450–487 | 490 | 502 | 489 |
| O(1) | ··· | ··· | ··· | 585 | 603 | 576 |

[a]Reference 35–38.
[b]References 16, 22, 30, and 40.
[c]This study.
[d]Reference 39.
[e]Reference 42.

opposite phase and couple to the O(4) ion with large amplitude. In the O(2)+O(3) mode, the O(2) and O(3) ions oscillate in the same phase, and the O(4) ion has a small amplitude in the opposite phase. In the O(4) and O(1) mode with highest energy in this system, the O(4) and O(1) ions have the largest oscillations, but there is a mixing between them.

Table III shows the eigenvalues of the above modes against other experimental[35–39] and computational[16,22,30,40–42] data for similar systems. The data for Y123 is in the range of the other computational and experimental data, although except for the O(2)−O(3) mode the data are almost 10% below the experimental values. Previous studies also show a similar underestimation,[22,30,40] and the error seems to be due to the LDA calculation. An exact study[16] has indicated that better agreement will be found in the optimized unit cell. However, because of the underestimation of LDA in determining the optimized structure, the LDA calculation of optimized unit cell is similar to the effect of pressure on the unit cell. So, this agreement could be explained as the effect of the mechanical pressure on the Raman data rather than the improvement of the computational method. Our data for Y124 indicate that except for Cu(2) mode the computational error has been decreased relative to Y123. Also, comparison between experiment and calculation in this system indicates that there is small overestimation in two modes. So, it seems that although LDA calculation has some error in determining the phonon eigenvalues, the error values depend on the compound's details.

### B. Electron-phonon interaction

We have calculated the electronic BS for the equilibrium and changed ionic positions of each bare $A_g$ Raman modes for the Y123 and Y124 systems. Due to the simplicity of the calculations, the position of one ion in each Raman mode has been changed and other ions have been remained fixed. As far as we know, the ionic position dependence of BS for Y124 has not been published yet, but some data are available for Y123. In addition, this study as an alternative method has focused on the role of electron-phonon interaction in both systems, which has not been considered well in the literature. We first discuss the results of Y124 and then present the results of Y123.

Figure 1 shows the BS and total density of state (TDOS) of Y124 system relative to the Fermi energy ($E_F$). The total shape of BS and details of the valence bands are very similar to the previous BS results for the Y124 system.[43,44] As expected from the similarities between the crystal structure of Y123 and Y124, the total shapes of the BS and TDOS of the two systems are nearly similar. The most important structural difference is the existence of two adjacent CuO chains in Y124 system which causes the unit cell of this system to be twice the unit cell of Y123. So, the number of ions in the

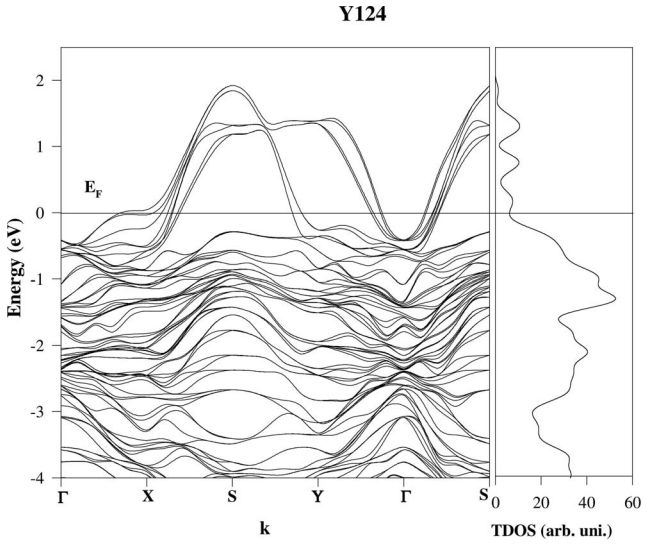


FIG. 1. The electronic BS including double degeneracy and corresponding TDOS for Y124 system near the Fermi energy.

considered unit cell of Y124 in this study (30 ions) is almost twice larger than the number of ions in the Y123 unit cell (13 ions), and hence, the total number of bands for Y124 is almost twice the total number for Y123. Because of the weak interaction between upper and lower half of the considered unit cell of Y124, the bands have nearly double degeneracy and have the same behavior under the change of ionic position. In the following, we refer only to one of these double degenerate bands.

The Y124 electronic BS, like in Y123, includes four separate parts related in order to the semicore O $2s$ and Ba $5p$ bands, respectively, at binding energies about −17 and −11 eV, valence bands of Cu $3d-$O $2p$ hybridization, and Y $4d$ and Ba $6s$ exited bands. Fourty-four Cu $3d-$O $2p$ valence bands have been distributed in the −7 to +2 eV range relative to the $E_F$. This system shows metallic behavior, and four bands intersect the Fermi energy, like for Y123 [hereafter, these bands are labeled as band numbers 1–4 (BN1–4)]. The BN3 and BN4 bands with the largest dispersions ( ~2.5 eV) crossing $E_F$ on $XS$ and $Y\Gamma$ are associated with the two dimensional antibonding states mainly due to hybridization of Cu$d_{x2-y2}$ and O$p_x$,$p_y$ of the $CuO_2$ planes. The less dispersive BN1 and BN2 bands (~1.9 eV) crossing $E_F$ on $XS$ and $SY$ are one dimensional antibonding of Cu$d_{x2-z2}$ and O$p_y$ hybridization in the CuO chain. The bands are nearly degenerate two by two for the $CuO_2$ planes and CuO chains, as it can be seen from Fig. 1. One important difference between these bands and those for Y123 is that the lowest dispersive band intersected Fermi level in Y123 (BN1 shown in Fig. 4), with a small hole pocket near the $S$ point,[45] lies completely below the Fermi level in Y124. The total shape and the amount of dispersion for the three other bands are nearly similar to the bands for Y123. The detail data for Y123 and their comparison with the other computational methods have been already published.[45] Finally, the very good agreement between the results of our calculation and the other computational methods based on the full-potential methods such as LAPW and LMTO[15,23,43–46] indicates that the pseudopotential VASP code has good accuracy for the band structure calculation of HTSC systems. Because of saving considerable computational time in this method, it could have some advantages to the full-potential method especially in performing large computational studies.

To determine the ionic position dependence of the electronic BS, band structure calculations have been carried out in different Raman modes in this system. In each calculation, the $z$ position of the considered ion has been changed, while the other ions have been fixed at their equilibrium positions. Figure 2 shows typical results of the ionic position dependence of BN3 for Cu(2), O(1), O(3), and O(4) displacements of Y124. For brevity, the results for the other bands have been not presented, although Fig. 3 will present all the results in a more comprehensive method. The BS changes continuously with ionic position and so just the largest and the smallest $z$ ionic position values of each displacement are shown in the figure. The obtained changes for Ba mode is small, and the changes for the O(2) and O(3), having nearly the same position in the compound, are also nearly the same.

The interesting result of the calculation is the strong ionic position dependence in some parts of these bands, while

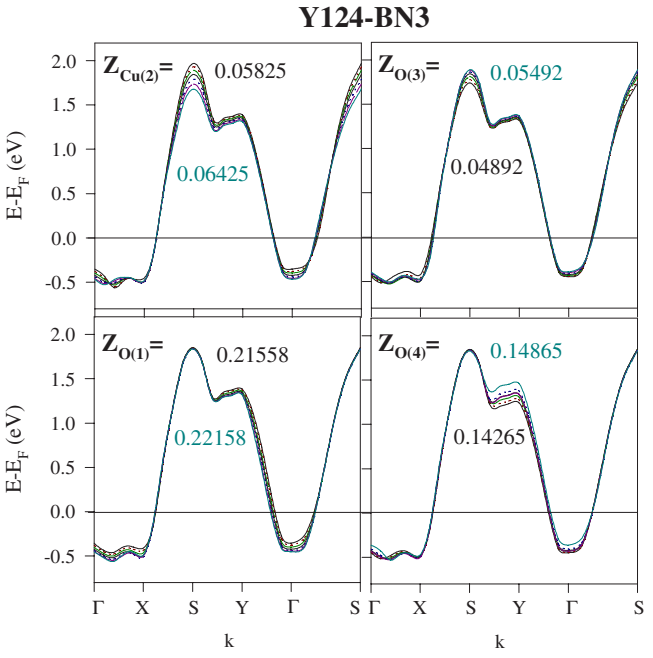


FIG. 2. (Color online) Changes of the BN3 by the change of $z$ ionic positions of Cu(2), O(1), O(3), and O(4) in Y124. In each calculation, the $z$ position of the considered ion has been changed, while the other ions have been fixed in their equilibrium positions. Due to the continuous change of BS with $z$ ionic position, only their largest and smallest values of the $z$ ionic positions are shown in the figure beside the corresponding curves.

other parts have been changed little or remained constant. For the Cu(2) displacements, the most important changes are near the $S$ point of BN3 (1.78 eV/Å) and BN4 (1.71 eV/Å), and the $X$ point of BN4 (1.1 eV/Å), while other parts have been changed little. Creation of hole carriers with decreasing $z$Cu(2) at the $X$ point of BN4 [similar to Y123 (Ref. 45)] indicates resonance of the hole concentration with this phonon mode which could be important for the superconducting properties. These changes for the O(3) and O(1) displacements are relatively small, but the changed regions could indicate which parts of the bands (partial bands) are related to the $CuO_2$ or CuO chains, respectively. For the O(3) displacement, BN1 and BN2 have not been changed much, while the most important changes occur in the $S$ point of BN3 and BN4. Compared with Y123,[45] there is no hole carrier creation or annihilation by the change of O(3) ionic position. For O(1), the changes have been occurred in the left shoulder of BN1 and the right shoulder of BN3.

For O(4) mode including large changes for all bands, the $S$ point of BN1 (1.35 eV/Å) and BN2 (1.33 eV/Å), the $Y$ point of BN3 (1.33 eV/Å) and BN4 (1.33 eV/Å), and the $X$ point of BN4 have been changed considerably. It resulted that in contrast to Y123 (shown below), the changes near the $X$ point of BN4 do not create or annihilate any holes in this band. The changes of the bands with the O(4) position is nearly half of the value for Y123. This could be due to the existence of only one O(4) ion near each CuO chain in Y124, while there are two O(4) ions near the CuO chains in Y123, which make a stronger hybridization with this band. Parts of these bands that have larger change with the O(4) displace-

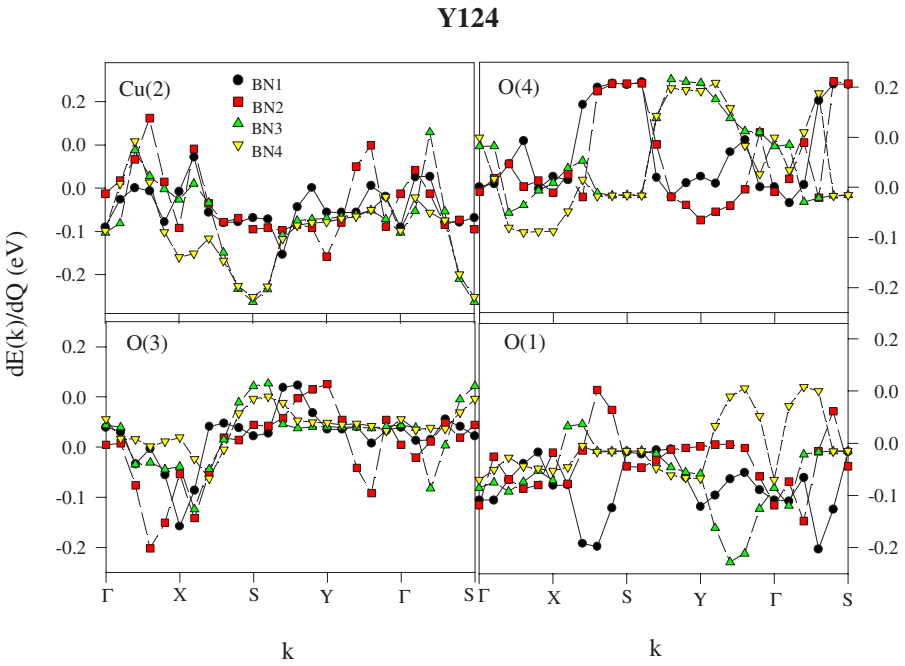


FIG. 3. (Color online) The derivative of the bands BN1–BN4 with respect to the phonon dimensionless coordinate $Q$ for the Cu(2), O(4), O(3), and O(1) ions of Y124.

ment indicate the partial band due to the Cu(1)−O(1)−O(4) hybridization, which is in agreement with previous calculations.[46]

To show better the ionic position dependence of the corresponding bands, we have calculated the derivative of the shift of top of the corresponding band (BN1–BN4) with respect to the $E_F$ (in eV unit) relative to the dimensionless phonon coordinate $Q$. $Q$ is derived from $Q\mathbf{e}_{\alpha\zeta} = (M_\alpha \omega_\zeta / h)^{1/2}\, \mathbf{u}_{\alpha\zeta}$ relation,[47] where $h$ is the Planck constant, $M_\alpha$ is the mass of ion $\alpha$, $\omega_\zeta = 2\pi f_\zeta$ and $f_\zeta$ is the frequency of $\zeta$ mode, $\mathbf{u}_{\alpha\zeta}$ is the corresponding real displacement of ion $\alpha$ in the $\zeta$ mode, and $\mathbf{e}_{\alpha\zeta}$ is the normalized eigenvector of the phonon mode (Tables I and II). Table IV shows the absolute value of the results for the Y124 system. By introducing $Q$, it would be easy to compare the results for different modes independent of the specific ions. Because of the existence of two tops for the BN3 and BN4 bands near $S$ and $Y$ points, we have considered both of them for these two bands. As can be seen from this table, the changes are small for Ba and O(1) ions while they are considerably large for the O(4), Cu(1), and Cu(2) ions. For the O(4) mode, considerable changes have been occurred near the $S$ point of BN1 and BN2 (0.21 eV) and $Y$ point of BN3 and BN4 (0.21 eV). For the Cu(2) mode, the changes are highest at $S$ point of BN3 and BN4 (0.25 eV) and at the $S$ point of BN1 (0.15 eV). For Cu(1), same as O(4), most changes have been occurred at the $S$ point of BN1 and BN2 (0.18 eV) and $Y$ point of BN3 and BN4 (0.19 eV). In Table IV, the $dN(E_F)/dQ$ for different modes are also presented [due to double degeneracy of the bands, the data have been divided by the factor 2 to obtain the real $N(E_F)$ for Y124 unit cell]. The $N(E_F)$ has large positive changes over $Q$ for Cu(2) and O(1), while it is negative for O(3) and O(4). These data are also another evidence for the strong ionic position dependence of the electronic structure for these systems.

To see more clearly the changes of the electronic band structure with ionic positions, we have calculated the derivative of the $E(k)$ over phonon dimensionless coordinate $Q$. The results for the bands BN1–BN4 for the Cu(2), O(4), O(3), and O(1) ions of the Y124 system are presented in Fig. 3. From this figure, the details of the changes of electronic band structure versus $k$ in each mode are clearly evident.

TABLE IV. The derivative values of the absolute value of shift of the top of the corresponding band (BN1–BN4) with respect to the Fermi energy (eV unit) and the density of states at $E_F$ relative to the dimensionless phonon coordinate $Q$ for Y124. For BN3 and BN4, the data have been calculated at both $S$ and $Y$ points.

| Ion | BN1 | BN2 | BN3 ($S$) | BN3 ($Y$) | BN4 ($S$) | BN4 ($Y$) | $dN(E_F)/dQ$ |
|---|---|---|---|---|---|---|---|
| Ba | 0.055 | 0.061 | 0.046 | 0.056 | 0.047 | 0.062 | 0.28 |
| Cu(2) | 0.154 | 0.095 | 0.263 | 0.070 | 0.252 | 0.079 | 1.30 |
| Cu(1) | 0.175 | 0.178 | 0.037 | 0.190 | 0.038 | 0.188 | 0.69 |
| O(2) | 0.020 | 0.036 | 0.108 | 0.032 | 0.089 | 0.028 | −0.26 |
| O(3) | 0.027 | 0.042 | 0.127 | 0.041 | 0.100 | 0.048 | −0.87 |
| O(4) | 0.210 | 0.207 | 0.015 | 0.208 | 0.016 | 0.208 | −0.78 |
| O(1) | 0.021 | 0.047 | 0.014 | 0.059 | 0.015 | 0.068 | 1.15 |

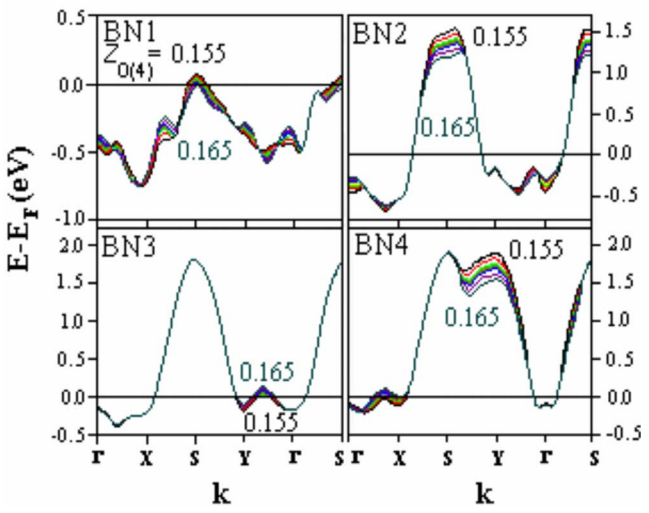


FIG. 4. (Color online) Changes of the four bands intersecting the Fermi energy by the change of $z$O(4) in Y123. Due to the continuous change of BS with $z$ ionic position, only their largest and smallest values of the $z$O(4) are shown in the figure beside the corresponding curves.

The strong ionic position dependence of the electronic BS results in strong ionic characterization of the bands which could indicate a strong interaction between electrons and phonons in this system. This result is in the direction of the experimental and computational studies which believe in the existence of a strong electron-phonon interaction in HTSC compounds.[6–11,14,22] Our calculations indicate that the changes are very anisotropic, and most changes have been occurred in the nodal $S(\pi,\pi)$ and antinodal $X(0,\pi)$ or $Y(\pi,0)$ directions of the Fermi surface. As can be seen from Figs. 2 and 3, the greatest changes are for the O(4) and Cu(2) modes and the least changes are for the Ba modes. This reveals the most important phonon modes for these changes.

Similar calculations for the Y123 system have resulted again the strong ionic position dependence of the BS, similar to the Y124 results. Figure 4 shows typical results for this system for the O(4) displacements. Similar to Y124, the changes for Ba are not much, and the changes for O(2) and O(3) are nearly the same. Some special parts of these bands have been changed much by the ionic displacement while the other parts are nearly unchanged.

The largest change in the Y123 bands is for the O(4) mode. In this mode, the $S$ point of BN1 (0.68 eV/Å) and BN2 (2.70 eV/Å), the $Y$ point of BN3 and BN4 (2.89 eV/Å), and the $X$ point of BN1 (1.6 eV/Å) and BN4 (1.3 eV/Å) have been changed considerably. It can also be seen that the changes near the $S$ point of BN1 annihilate hole carriers by the increase of $z$O(4), while close to the $Y$ point of BN3 and the $X$ point of BN4 hole carriers are created by the increase of $z$O(4). For the Cu(2) displacements, most important changes are near the $S$ point of BN1, BN3 (2.29 eV/Å), and BN4 (2.20 eV/Å), and the $X$ point of BN4 (1.3 eV/Å), while the intermediate parts have not been changed much. For the $S$ point of BN1 and the $X$ point of BN4, we see the creation of hole carriers with the decrease of $z$Cu(2), which could be important for the superconducting properties in this system. This indicates that the number of holes could resonate with this phonon mode. The results for the O(3) displacements are somehow different: The BN1 and BN2 have not been changed much, while most important changes are at the $S$ point of BN3 (1.49 eV/Å) and BN4 (1.27 eV/Å). In this mode, little hole carrier is created near the $S$ point of BN1 and the $Y$ point of BN3 by the decrease of $z$O(3).

Similar data as in Table IV have been calculated for the Y123 system and summarized in Table V. Again, we see that there are large changes of band widths over $Q$ for O(4), Cu(2), and O(3), which indicates their important roles in the electronic structure of this system. For O(4), most changes are for the $S$ point of BN2 (0.40 eV) and $Y$ point of BN4 (0.43 eV), while for Cu(2) and O(3), respectively, most changes for the $S$ point of BN3 are 0.29 and 0.19 eV, and of BN4 are 0.28 and 0.17 eV. Large changes of $N(E_F)$ with O(4) ion also indicate the important effect of this ionic position in the electronic properties of this system.

Our calculations clearly indicate that the electronic BS has been changed strongly with the ionic displacement in Y123 and Y124 systems. Large changes such as 2.9 eV/Å for Y123 and 1.8 eV/Å for Y124 indicate a strong ionic characterization of the electronic BS of both systems. As it has been resulted from the tight-binding calculation of Y123 system,[48] the amplitude of the bands—from the top to bottom of the bands, related to the $CuO_2$ plane and CuO chain[15]—are roughly proportional to the Cu(2)−O(2) and O(3), and Cu(1)−O(1) and O(4) hopping integrals, $t$ and $t'$, respectively. The changes of $z$O(2) and $z$O(3) and $z$O(4) change the Cu(2)−O(2) and O(3) and Cu(1)−O(4) bond lengths, respectively. So, from this study, it is concluded that the hoping parameter $t$ and $t'$ are strongly dependent on the

TABLE V. The derivative values of the absolute value of the shift of the top of the corresponding band (BN1–BN4) with respect to the Fermi energy (eV unit) and the density of states at $E_F$ relative to the dimensionless phonon coordinate $Q$ for Y123. For BN4, the data have been calculated at both $S$ and $Y$ points.

| Ion | BN1 | BN2 | BN3 ($S$) | BN4 ($S$) | BN4 ($Y$) | $dN(E_F)/dQ$ |
|---|---|---|---|---|---|---|
| Ba | 0.024 | 0.016 | 0.043 | 0.044 | 0.035 | 0.34 |
| Cu(2) | 0.082 | 0.136 | 0.291 | 0.280 | 0.088 | 0.48 |
| O(2) | 0.022 | 0.025 | 0.135 | 0.109 | 0.027 | −0.33 |
| O(3) | 0.042 | 0.056 | 0.195 | 0.167 | 0.061 | −0.35 |
| O(4) | 0.102 | 0.402 | 0.010 | 0.016 | 0.431 | −2.04 |

ionic distances in both of the $CuO_2$ plane and CuO chains in this system, which can be considered to interpret the experimental results related to the electron-phonon interaction. For example, the large changes of the $t$ have been applied to explain the strong renormalization of the half-breathing mode.[13,49]

Also, these calculations conclude the strong anisotropic dependence of the electronic BS to the ionic position in the $A_g$ Raman modes. Our paper is quantized well to indicate the strong ionic dependence of the electronic band structure, and as a result, strong change of hopping parameter. Although the calculated data are not sufficient for calculating the strength of the electron-phonon coupling, there are some experimental[6,7,9,10] and theoretical[8,13,14] evidences indicating a strong electron-phonon interaction in the HTSC systems (see Introduaction for details). Our computational data qualitatively support the idea that hole carriers could couple with phonons and present the most important part of the Birilluion zone that could be considered in the experimental data interpretation.

## IV. CONCLUSIONS

The relative differences of the calculated equilibrium lattice parameters and volumes with the experimental data have been derived, respectively, to be −1.14% and −3.5% for the Y123 and Y124 systems, which are optimized relative to the LAPW method in LDA. The calculated eigenfrequencies and eigenvectors of $A_g$ Raman modes and electronic BS for both systems are in good agreement with the experimental and computational data. These calculations not only indicate the capability of the VASP code in determining the equilibrium lattice parameters, and phonon and electronic structure calculations in the LDA approach for HTSC compounds but also save considerable computational time for these calculations. Large changes of the electronic BS with ionic position (as large as 2–3 eV/Å) indicate an important ionic position dependence and strong ionic characterization of the electronic BS in both systems, which suggest a strong electron-phonon interaction in these systems. The largest change is related to the Cu(2) and O(4) ions, which indicates that the related phonon modes can, affect strongly the electronic structure of these systems. The changes are completely anisotropic, such that the biggest changes have been occurred in some special points of the $k$ space such as $X$, $Y$, and $S$.

## ACKNOWLEDGMENTS

We wish to thank A. Tavana, C. Ambrosch-Draxl, and E. Ya. Sherman for useful discussions. This work was supported in part by the Offices of the Vice President for Research and Dean of Graduate Studies at Sharif University of Technology.

*Corresponding author.
FAX: 98 21 66012983. akhavan@sharif.edu

[1] J. G. Bednorz and K. A. Mueller, Z. Phys. B: Condens. Matter **64**, 189 (1986).
[2] M. L. Kulic, Phys. Rep. **338**, 1 (2000).
[3] A. Damascelli, Z.-X. Shen, and Z. Hussain, Rev. Mod. Phys. **75**, 473 (2003).
[4] P. B. Allen, in *Physical Properties of High Temperature Superconductors*, edited by D. M. Ginsberg (World Scientific, Singapore, 1989), Vol. 1, p. 213.
[5] J. P. Franck, in *Physical Properties of High Temperature Superconductors*, edited by D. M. Ginsberg (World Scientific, Singapore, 1994), Vol. 4, p. 189.
[6] A. Lanzara, P. V. Bogdanov, X. J. Zhou, S. A. Kellar, D. L. Feng, E. D. Lu, T. Yoshida, H. Eisaki, A. Fujimori, K. Kishio, J.-I. Shimoyama, T. Noda, S. Uchida, Z. Hussain, and Z.-X. Shen, Nature (London) **412**, 510 (2001).
[7] G.-H. Gweon, T. Sasagawa, S. Y. Zhou, J. Graft, H. Takagi, D.-H. Lee, and A. Lanzara, Nature (London) **430**, 187 (2004).
[8] M. L. Kulic and O. V. Dolgov, Phys. Rev. B **71**, 092505 (2005).
[9] R. J. McQueeney, Y. Petrov, T. Egami, M. Yethiraj, G. Shirane, and Y. Endoh, Phys. Rev. Lett. **82**, 628 (1999).
[10] H. Uchiyama, A. Q. R. Baron, S. Tsutsui, Y. Tanaka, W.-Z. Hu, A. Yamamoto, S. Tajima, and Y. Endoh, Phys. Rev. Lett. **92**, 197005 (2004) and references therein.
[11] T. Fukuda, J. Mizuki, K. Ikeuchi, K. Yamada, A. Q. R. Baron, and S. Tsutsui, Phys. Rev. B **71**, 060501(R) (2005).
[12] G.-M. Zhao, H. Keller, and K. Conder, J. Phys.: Condens. Matter **13**, R569 (2001).
[13] O. Rosch and O. Gunnarsson, Phys. Rev. Lett. **92**, 146403 (2004).
[14] H. Krakauer, W. E. Pickett, and R. E. Cohen, Phys. Rev. B **47**, 1002 (1993).
[15] W. E. Pickett, Rev. Mod. Phys. **61**, 433 (1989).
[16] R. Kouba and C. Ambrosch-Draxl, and B. Zangger, Phys. Rev. B **60**, 9321 (1999).
[17] E. G. Maksimov, S. N. Rashkeev, S. Yu. Savrasov, and Yu. A. Uspenskii, Phys. Rev. Lett. **63**, 1880 (1989).
[18] C. Ambrosch-Draxl, R. Abt, and P. Knoll, Physica C **235-240**, 2119 (1994).
[19] J. Zaanen, M. Alouani, and O. Jepsen, Phys. Rev. B **40**, 837 (1989).
[20] C. Ambrosch-Draxl, H. Auer, R. Kouba, E. Ya. Sherman, P. Knoll, and M. Mayer, Phys. Rev. B **65**, 064501 (2002).
[21] E. T. Heyen, S. N. Rashkeev, I. I. Mazin, O. K. Andersen, R. Liu, M. Cardona, and O. Jepsen, Phys. Rev. Lett. **65**, 3048 (1990).
[22] C. O. Rodriguez, A. I. Liechtenstein, I. I. Mazin, O. Jepsen, O. K. Andersen, and M. Methfessel, Phys. Rev. B **42**, 2692 (1990).
[23] H. Khosroabadi, B. Mossalla, and M. Akhavan, Phys. Rev. B **70**, 134509 (2004).
[24] H. Kim and J. Ihm, Phys. Rev. B **51**, 3886 (1995).
[25] P. Blaha, K. Schwarz, G. K. H. Madsen, D. Kvasnicka, and J. Luitz, Wien2k, an augmented plane wave + local orbitals program for calculating crystal properties, Karlheniz Schwarz, Technische Universitat Wien, Austria, 2001.
[26] G. Kresse and J. Furthmuller, Comput. Mater. Sci. **6**, 15 (1996).

[27] G. Kresse and J. Furthmuller, Phys. Rev. B **54**, 11169 (1996).
[28] R. M. Hazen, in *Physical Properties of High Temperature Superconductors*, edited by D. M. Ginsberg (World Scientific, Singapore, 1990), Vol. 3, Chap. 3.
[29] H. J. Monkhorst and J. D. Pack, Phys. Rev. B **13**, 5188 (1976).
[30] H. Khosroabadi, A. Tavana, and M. Akhavan, Eur. Phys. J. B **51**, 161 (2006) and references therein.
[31] R. E. Cohen, W. E. Pickett, and H. Krakauer, Phys. Rev. Lett. **62**, 831 (1989).
[32] X. J. Chen, C. D. Gong, and Y. B. Yu, Phys. Rev. B **61**, 3691 (2000).
[33] J. D. Jorgensen, S. Pei, P. Lightfoot, D. G. Hinks, B. W. Veal, B. Dabrowski, A. P. Paulikas, and R. Kleb, Physica C **171**, 93 (1990).
[34] O. V. Misochko, E. I. Rashba, E. Ya. Sherman, and V. B. Timofeev, Phys. Rep. **194**, 387 (1990).
[35] C. Thomsen and M. Cardona, in *Physical Properties of High Temperature Superconductors*, edited by D. M. Ginsberg (World Scientific, Singapore, 1989), Vol. 1, p. 409.
[36] T. Strach, T. Ruf, E. Schönherr, and M. Cardona, Phys. Rev. B **51**, 16460 (1995).
[37] G. Burns, F. H. Dacol, F. Holtzberg, and D. L. Kaiser, Solid State Commun. **66**, 217 (1988).
[38] K. F. McCarty, J. Z. Liu, R. N. Shelton, and H. B. Radousky, Phys. Rev. B **41**, 8792 (1990).
[39] E. T. Heyen, R. Liu, C. Thomsen, R. Kremer, M. Cardona, J. Karpinski, E. Kaldis, and S. Rusiecki, Phys. Rev. B **41**, 11058 (1990).
[40] C. Ambrosch-Draxl, R. Kouba, and P. Knoll, Z. Phys. B: Condens. Matter **104**, 687 (1997).
[41] H. Khosroabadi, B. Mossalla, and M. Akhavan, Phys. Status Solidi C **3**, 3140 (2006).
[42] M. Cardona, Physica C **317-318**, 30 (1999).
[43] T. Oguchi, T. Sasaki, and K. Terakura, Physica C **172**, 277 (1990).
[44] J. Yu, K. T. Park, and A. J. Freeman, Physica C **172**, 467 (1990).
[45] H. Khosroabadi and M. Akhavan, Phys. Status Solidi C **1**, 1863 (2004).
[46] C. Ambrosch-Draxl, P. Blaha, and K. Schwarz, Phys. Rev. B **44**, 5141 (1991).
[47] J. Spitaler, E. Ya. Sherman, and C. Ambrosch-Draxl, Phys. Rev. B **75**, 014302 (2007).
[48] J. Zaanen, A. T. Paxton, O. Jepsen, and O. K. Andersen, Phys. Rev. Lett. **60**, 2685 (1988).
[49] O. Rosch and O. Gunnarsson, Phys. Rev. B **70**, 224518 (2004).